MR, ^{18}F-FDG, and ^{18}F-AV45 PET Correlate With AD *PSEN1* Original Phenotype

Laure Saint-Aubert, MSc,† Pierre Payoux, MD, PhD,*†‡ Didier Hannequin, MD, PhD,§ Emmanuel J. Barbeau, PhD,‖ Dominique Campion, MD, PhD,§ Marie-Bernadette Delisle, PhD,¶# Mathieu Tafani, MD,†‡ Gérard Viallard,*† Patrice Péran, PhD,*† Michèle Puel, MD, PhD,*†** François Chollet, MD, PhD,*†** Jean-François Demonet, MD, PhD,†† and Jérémie Pariente, MD, PhD*†***

Abstract: We report the case of a 37-year-old man suffering from insidious visual agnosia and spastic paraparesis due to a *PSEN1* mutation. His mother was diagnosed with Alzheimer disease after a biopsy. He was assessed by multimodal neuroimaging, including new in vivo positron emission tomography amyloid imaging (^{18}F-AV45). His data were compared with those from healthy participants and patients with sporadic predemential Alzheimer disease. He exhibited posterior cortical thickness reduction, posterior hypometabolism, and increased amyloid ligand uptake in the posterior cortex and the striatum. We show that ^{18}F-AV45 positron emission tomography allows visualization of the unusual pattern of amyloid deposits that co-localize with cortical atrophy in this genetic form of Alzheimer disease.

Key Words: Alzheimer disease, amyloid, AV45, genetics, MRI, PET

(*Alzheimer Dis Assoc Disord* 2013;27:91–94)

Presenilin-1 (*PSEN1*) mutation is the most frequent cause of familial Alzheimer disease (AD). To date, 185 *PSEN1* mutations have been discovered (http://www.molgen.ua.ac.be/ADMutations). The variant of AD with spastic paraparesis (SP) has been associated with 25 *PSEN1* mutations. Only 2 studies have investigated in vivo amyloid deposition in patients with familial AD and SP related to *PSEN1* mutations.[1,2] We report the case of a young patient suffering from AD and SP related to a *PSEN1* mutation assessed by a multimodal neuroimaging study, including amyloid positron emission tomography (PET) imaging (^{18}F-AV45).

Received for publication June 8, 2011; accepted September 27, 2011.

From the *Inserm, Imagerie Cérébrale et Handicaps Neurologiques; †Université de Toulouse, UPS, Imagerie Cérébrale et Handicaps Neurologiques UMR 825, F-31059; ‡Service de Médecine Nucléaire, Pôle Imagerie, University Hospital Purpan; **Service de Neurologie, Pôle Neurosciences, University Hospital Purpan; ‖Université de Toulouse, UPS, Centre de Recherche Cerveau et Cognition, CNRS, CerCo; ¶Service d'Anatomie Pathologique et Histologie-Cytologie, CHU Rangueil-Larrey, Toulouse, France; #INSERM U 858, Faculté de Médecine Rangueil, UPS, Toulouse; §INSERM U 164, CNR-MAJ, Faculté de Médecine, Rouen; Département de Neurologie, CHU Rouen, Rouen cedex, France; and ††Leenaards Memory Center, CHUV & University of Lausanne, Switzerland.

Supported by the ANR (Agence Nationale de la Recherche) "iPAD" ANR-08-JCJC-0040 and AOL 2007 No. 07 306 02 and approved by the local ethics committee.

The authors declare no conflicts of interest.

Reprints: Jérémie Pariente, MD, PhD, Inserm, Imagerie Cérébrale et Handicaps Neurologiques UMR 825, CHU Purpan, Place du Dr Baylac, F-31059 Toulouse Cedex 9, France (e-mail: jeremie.pariente@inserm.fr).

CASE STUDY

ErA, a 37-year-old man, attended our outpatient clinic for a progressive gait disorder, having 18 months' history, followed by cognitive difficulties. SP was diagnosed clinically. His mini mental state examination was at 22/30, and the frontal assessment battery at 14/18. Severe aperceptive visual agnosia was revealed by very poor confrontation naming performance involving visual errors and impossible copying of the Rey figure. Story recall from the MEM3 was impaired (see Lezak[3] for test references). Within a year, ErA's sight became restricted to the perception of large, strongly contrasted shapes. His behavior and mood were not affected, although joviality was reported. A clinical structural magnetic resonance imaging (MRI) scan showed posterior cortical atrophy on T1 sequence (Fig. 1Aa), but neither white matter lesion nor microhemorrhage on T2 and T2* images.

Cerebrospinal fluid analysis showed increased τ and phospho-τ markers, and decreased Aβ42 (708, 105, and 187 pg/mL, respectively, whereas normative values are $\leq$450, $\leq$50, and $\geq$500 pg/mL, respectively; INNOTEST, Innogenetics), suggesting AD. In addition, ErA's genomic DNA was isolated from blood lymphocytes. The entire coding sequence and the exon/intron boundaries of *PSEN1* were sequenced as described previously.[4] A *PSEN1* mutation c.668A > G, p.Gln223Arg was found in exon 7.

ErA underwent a 3D-T1 structural MRI scan, ^{18}F-fluorodeoxyglucose (^{18}F-FDG), and florbetapir (^{18}F-AV45) PET scans. Images were acquired for 10 minutes, 30 minutes after FDG injection, and for 20 minutes, 50 minutes after AV45 injection (Figs. 1Ab and c). We recruited 10 elderly healthy controls (mean age: 68.2 ± 3.6 y, level of education: 13.1 ± 3.8) and 11 predemential AD patients[5] (mean age: 72.1 ± 4.8 y, level of education: 12.1 ± 2.8). AD patients and healthy controls underwent the same imaging protocol. All patients gave their informed consent before any examination. Furthermore, 3D-T1 MRI scans from a group of 18 healthy participants matched in age with ErA (mean age: 36.8 ± 4.1 y) were collected from the Oasis database (http://www.oasis-brains.org/).

From 3D-T1 MRI scans, the cortical thickness was measured for all subjects using a software developed in our laboratory.[6] Mean values and standard deviations (SDs) were obtained in all Brodmann areas (BA) for the AD

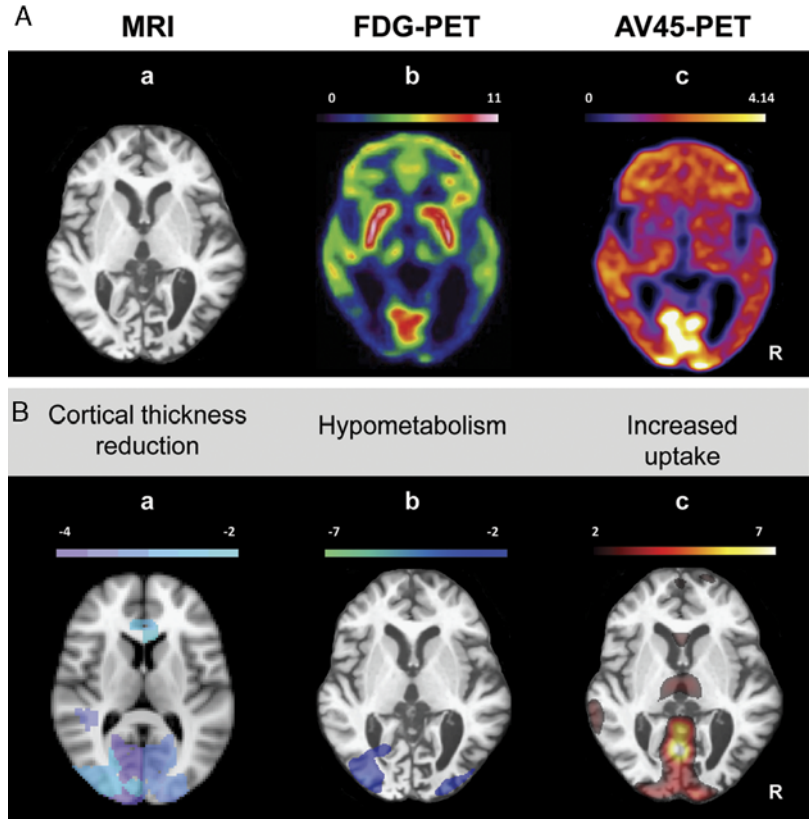

FIGURE 1. ErA's structural magnetic resonance imaging (MRI), ^{18}F-fluorodeoxyglucose (FDG), and ^{18}F-AV45 positron emission tomography (PET) imaging and group comparisons. R indicates the right hemisphere. A, ErA's images: (a) structural MRI, axial slice; (b) ^{18}F-FDG. Color scale indicates standard uptake values; (c) ^{18}F-AV45 PET. Color scale indicates standard uptake values. B, Comparison of ErA and the control groups: (a) cortical thickness comparison between ErA and a group of 18 healthy age-matched controls. ErA's cortical atrophy below −2 SD is shown; (b) comparison of ^{18}F-FDG images between ErA and a group of 11 Alzheimer disease patients. ErA's hypometabolism below −2 SD is shown; (c) comparison of ^{18}F-AV45 PET images between ErA and a group of 11 Alzheimer disease patients. ErA's higher amyloid retention above 2 SD is shown.

patients, the age-matched, and the elderly control groups. ErA was compared with each of them using Z scores.

PET images were whole brain normalized using the PET template from the Statistical Parametric Mapping software, version 8 (SPM8), for FDG and AVID's template (http://www.avidrp.com/) for AV45, and were smoothed ($8 \times 8 \times 8$ mm for FDG, $10 \times 10 \times 10$ mm for AV45). For the 2 PET examinations, mean and SDs images were obtained for both the AD patients and the healthy elderly control groups, using SPM8. ErA was compared with both groups using Z scores. All Z scores below −2 or above 2 were considered as significant.

In the MRI study, ErA showed pervasive cortical thinning down compared with the healthy young control group (Fig. 1Ba). The greatest differences were found in the left occipital lobe (BA17, $Z = -3.14$), the right posterior cingular cortex (BA23, $Z = -3.39$), the left temporal lobe (BA20, $Z = -3.71$), and the left frontal lobe (BA11, $Z = -2.96$). Compared with the AD patients group, none of ErA's Z scores was below −2. Compared with the healthy elderly group, right BA17 was below −2 SD ($Z = -2.12$).

Regarding the FDG study, metabolism was found to be lower in ErA compared with the AD group in both right and left occipital cortices ($Z = -3.9$ and -4.2, respectively) (Fig. 1Bb). Conversely, ErA had a relatively higher metabolism in the frontal lobes (right: $Z = 2.7$ and left: $Z = 3.4$), the hippocampus (right: $Z = 2.6$ and left: $Z = 2.5$), and the striatum (right: $Z = 2.8$ and left: $Z = 3.5$). When compared with healthy elderly participants, ErA's metabolism was lower in the occipital lobes (right: $Z = -2.8$ and left: $Z = -3.8$). No Z score was found to be above 2.

Regarding the AV45 study, ErA showed a higher cortical retention than AD patients in the occipital lobes ($Z = 6.8$), the thalami ($Z = 2.8$; Fig. 1Bc), and the right striatum ($Z = 2.0$), but also in the hippocampus (right: $Z = 2.5$ and left: $Z = 2.7$) and the cerebellum (right: $Z = 6.8$ and left: $Z = 6.9$). No Z score was found to be below −2. Compared with the healthy controls, ErA's retention was spread across the whole cortex. No Z score was found to be below −2.

ErA's mother died at age 39. Clinical notes retrieved for her reported pyramidal syndrome and dementia. A frontal brain biopsy was reviewed and a complementary immunohistochemical study revealed the presence of cotton-wool plaques, a few neuritic and core-centered plaques, neurofibrillary tangles, and neuropil threads. There was no amyloid angiopathy in this small specimen (Fig. 2).

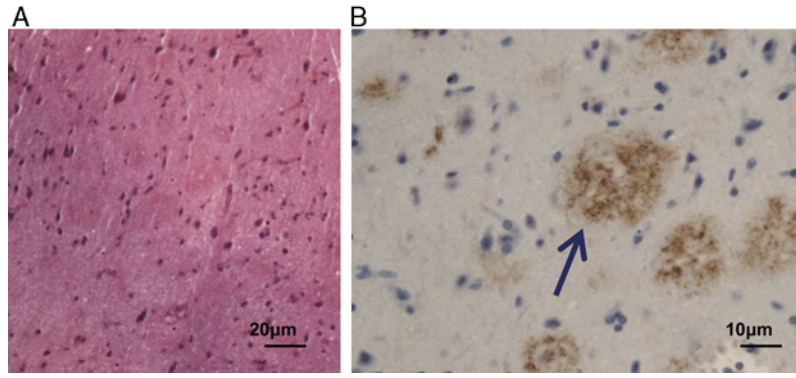

FIGURE 2. ErA's mother's brain biopsy (right frontal lobe). A, Some well-defined plaques are readily visible on routine staining (hematoxylin and eosin, ×200). B, Plaques were stained by an antibody directed against Aβ. Arrow shows a stained cotton-wool plaque (anti-Aβ, Dako, ^{6}F/3D, ×400).

DISCUSSION

We report the first case of a *PSEN1* mutation carrier who developed primary visual agnosia, as observed in the posterior cortical atrophy syndrome. Our MRI and PET findings showed that atrophy and hypometabolism were predominant in the occipital cortex bilaterally, but also that amyloid marker retention was higher in that region compared with sporadic predemential AD patients.

When comparing ErA and the group of age-matched controls, we observed a cortical thinning in ErA comparable to that we have described elsewhere in a predemential AD population.[6] It is important to note that this cortical atrophy was particularly marked in the occipital lobes for ErA, which is congruent with his symptoms. We did not find any relevant difference of atrophy between ErA and AD patients despite this severe occipital atrophy. ErA's cortex is thicker in various regions compared with the AD patients, and this may be due to the age difference. Besides, ErA and the group of elderly controls had different cortical thickness in only 1 BA. This slight difference is also probably due to the age difference between ErA and this control group.

We used a novel amyloid ligand, ^{18}F-AV45. It seems to have an excellent binding affinity to Aβ in the AD brain according to ex vivo autoradiography in transgenic AD model mice. This affinity seems higher than PiB's. AV45 specifically binds to Aβ in vitro and is a safe PET tracer for studying Aβ distribution in human brains. Recent publications suggest that AV45 is a sensitive marker of amyloid load in cortical gray matter in elderly individuals and can differentiate groups of subjects meeting the standard diagnostic criteria for AD, mild cognitive impairment, and normal cognitive functions.[7]

In our case, the main amyloid binding difference between ErA and AD patients was observed in the occipital lobes. This was also where the main hypometabolism was found. It thus seems that a close relationship exists in this particular case between the amyloid deposition pattern, the cortical damage as assessed by both functional and morphologic imaging, and the clinical presentation. Such concordance between modalities differs from what is classically observed, as neurofibrillary tangles correlate better with clinical symptoms than with amyloid pathology. A recent study has found similar results in atypical clinical variant of sporadic AD patients.[8] ErA's occipital amyloid uptake could partly account for cerebral amyloid angiopathy.[9] It is nevertheless hardly plausible as ErA's T2* MRI sequence was free from microhemorrhages.

We found that ErA had a relatively high, right-sided striatal AV45 uptake. This result is reported in previous PET amyloid imaging studies on *PSEN1* mutation carriers.[1,2] Klunk et al[1] also found a greater retention of PiB in the striatum in *PSEN1* patients compared with sporadic AD patients. Interestingly, in that study, asymptomatic mutation carriers exhibited PiB retention in the striatum only, suggesting that pathologic amyloid deposition may start in the striatum well before the onset of clinical symptoms. Koivunen et al[2] also found increased striatal PiB uptakes when comparing *PSEN1* mutation carriers with controls.

In this study, we also found an unexpected result: a higher bilateral hippocampal AV45 uptake was observed in ErA than in AD patients, whereas his hippocampal metabolism was lower. This pattern has not been described previously in *PSEN1* studies. In contrast, a recent study has shown correlations between PiB fixation and hippocampal atrophy in sporadic AD.[10] Our results also seem to be at odds with the idea that amyloid deposition is related with atrophy and symptoms that were put forward for occipital areas. Therefore, the relation between amyloid deposition and symptoms is complex and merits further analyses.

Cerebellar AV45 retention was observed in ErA. The cerebellum is generally believed to be spared by the amyloid pathology in sporadic AD. However, similar results have been found in 2 studies using PiB on *PSEN1* cases.[1,2] Pathologic studies have shown diffuse amyloid deposits in *PSEN1* patients presenting gait impairment like ErA.[11] This element is important as the cerebellum is often used as a reference region in PET imaging studies.[2,7]

In this case report, we confirm that AV45 PET is an important tool for imaging in vivo amyloid burden. The different patterns of AV45 binding found between our *PSEN1* patient and the group of sporadic AD patients demonstrate how the distribution of Aβ deposits can account for the heterogeneity of the AD phenotype.

ACKNOWLEDGMENTS

The authors thank Prof. Denis Guilloteau of Tours, France, for his help in developing the AV45 ligand.

REFERENCES

1. Klunk WE, Price JC, Mathis CA, et al. Amyloid deposition begins in the striatum of presenilin-1 mutation carriers from two unrelated pedigrees. *J Neurosci*. 2007;27:6174–6184.

2. Koivunen J, Verkkoniemi A, Aalto S, et al. PET amyloid ligand [^{11}C]PIB uptake shows predominantly striatal increase in variant Alzheimer's disease. *Brain*. 2008;131(Pt 7):1845–1853.
3. Lezak MD. *Neuropsychological Assessment*. New York, NY: Oxford University Press; 2004.
4. Raux G, Guyant-Marechal L, Martin C, et al. Molecular diagnosis of autosomal dominant early onset Alzheimer's disease: an update. *J Med Genet*. 2005;42:793–795.
5. Dubois B, Feldman HH, Jacova C, et al. Revising the definition of Alzheimer's disease: a new lexicon. *Lancet Neurol*. 2011;9:1118–1127.
6. Querbes O, Aubry F, Pariente J, et al. Early diagnosis of Alzheimer's disease using cortical thickness: impact of cognitive reserve. *Brain*. 2009;132(Pt 8):2036–2047.
7. Clark CM, Schneider JA, Bedell BJ, et al. Use of florbetapir-PET for imaging beta-amyloid pathology. *JAMA*. 2011;305:275–283.
8. Ng SY, Villemagne VL, Masters CL, et al. Evaluating atypical dementia syndromes using positron emission tomography with carbon 11 labeled Pittsburgh compound B. *Arch Neurol*. 2007; 64:1140–1144.
9. Johnson KA, Gregas M, Becker JA, et al. Imaging of amyloid burden and distribution in cerebral amyloid angiopathy. *Ann Neurol*. 2007;62:229–234.
10. Chetelat G, Villemagne VL, Bourgeat P, et al. Relationship between atrophy and beta-amyloid deposition in Alzheimer disease. *Ann Neurol*. 2010;67:317–324.
11. Anheim M, Hannequin D, Boulay C, et al. Ataxic variant of Alzheimer's disease caused by Pro117Ala PSEN1 mutation. *J Neurol Neurosurg Psychiatry*. 2007;78:1414–1415.

